Assessing the monitoring performance using a synthetic microseismic catalogue for hydraulic fracturing

J. A. López-Comino[1]*, M. Kriegerowski [1,2], S. Cesca [1], T. Dahm [1], J. Mirek [3] & S. Lasocki [3]

[1]*GFZ German Research Centre for Geosciences, Telegrafenberg, D-14473 Potsdam, Germany (*jalopez@gfz-potsdam.com)*

[2]*Universität Potsdam, Institut für Erd- und Umweltwissenschaften, 14476 Potsdam-Golm, Germany*

[3]*Institute of Geophysics, Polish Academy of Sciences, Krakow, Poland*

EGU2016-7031

1. INTRODUCTION

Hydraulic fracturing (HF) is considered among the human operations which could induce or trigger seismicity or microseismic activity. In order to assess the sensitivity of microseismicity to HF operations, we perform a seismic monitoring at a shale gas exploitation site in the central-western part of the Peribaltic synclise at Pomerania (Poland). The monitoring will be continued before, during and after the termination of hydraulic fracturing operations. The fracking operations are planned in May 2016 at a depth 4000 m. A specific network setup has been installed since summer 2015, including a distributed network of broadband stations and three small-scale arrays (figure 1). The network covers a region of 60 km2. The aperture of small scale arrays is between 450 and 950 m.

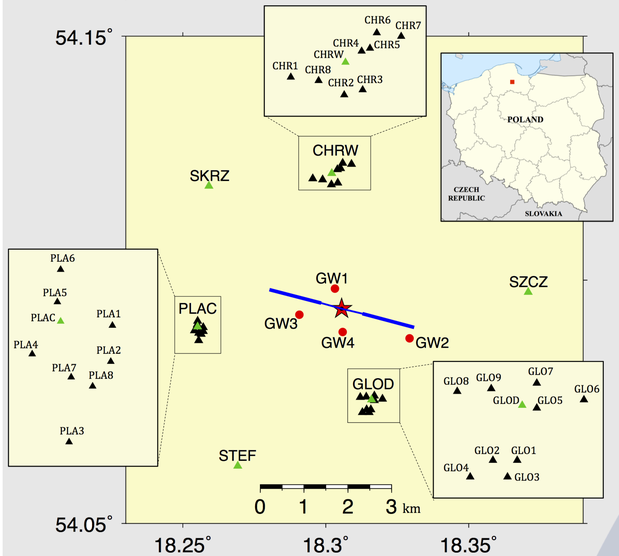

Figure 1. *Map of seismic monitoring composed of 6 broadband stations (green triangles), 3 small-scale arrays (inset boxes), each one composed of 8 to 9 short period stations (black triangles) and 4 shallow borehole stations (red circles). Fracking area (red star, vertical borehole) and horizontal drillings (blue lines) are shown. The inset map shows the fracking area (red square) in Poland.*

2. SYNTHETIC MICROSEISMIC CATALOGUE

We adopt a recently developed tool to generate a synthetic catalogue and waveform dataset, which realistically account for the expected microseismicity. Synthetic waveforms are generated for a 1D local crustal model (Grad et al., 2015), considering realistic distributions of hypocenters, magnitudes, moment tensors and source durations (figure 2). On the one hand, the regional tectonic in situ stress state controls the direction of hydraulic fracture growth in the unperturbed rock formation. Assuming double couple sources of random orientations, the rake is conditioned by the strike and dip of the rupture plane and the maximum horizontal compressive stress SH (15°, perpendicular to fracking drilling). On the other hand, processes involving rapid fluid injection can produce tensile failures with significant non-double-couple components, opening in the direction of the minimal compressive stress, and closing after the injection (Baig and Urbanic, 2010). To reproduce all these processes, we build a synthetic dataset with 4000 events divided in four families according different types of focal mechanisms: random full MT mechanism, double couples and positive and negative tensile cracks, consistent with the background stress.

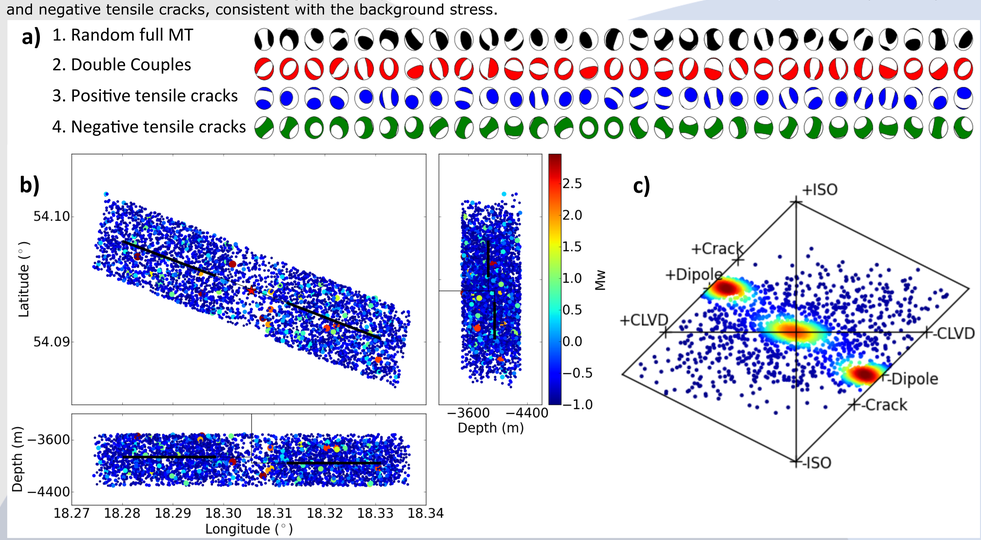

Figure 2*. a) Focal mechanism examples for the different families of expected microseismicity.*
b) Distribution of hypocenters and magnitudes for the synthetic microseismic catalogue in the fracturing area. We consider moment magnitudes between -1 and 3, the frequency-magnitude distribution follows a Gutenberg-Richter law with b = 1 and a = 1.84. The maximum rupture length (350 m) is calculated considering a circular fault model of Madariaga (1976) and a stress drop average = 2.7 MPa for earthquakes within the chosen magnitude range (Kwiatek et al., 2011). Durations sources are calculated assuming a rupture velocity = 0.9 S-wave velocity. Black lines show the fracking drillings.
c) Hudson source-type plot showing the Gaussian Kernel density for the complete synthetic microseismic catalogue where red denotes higher density and blue regions with few events

3. SYNTHETIC WAVEFORM ANALYSIS

Synthetic waveforms (figure 3) are generated with the Pyrocko package (http://emolch.github.io/pyrocko/). The maximum amplitudes of synthetuc full waveforms are discusssed in function of the hipocentral distance and the moment magnitude (figure 4). The amplitude increases exponentially with the magnitude; the effects of geometrical spreading are observed according to the hypocentral distance.

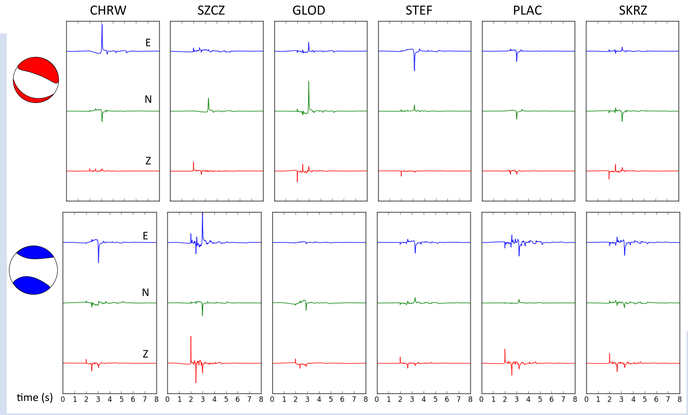

Figure 3. *Synthetic waveform examples (displacement) in the broadband stations for one double couple event with Mw = -0.5 [amplitude max = 2.42·10-9 m] (top) and one positive tensile crack event with Mw = 0 [amplitude max = 1.09·10-8 m] (bottom).*

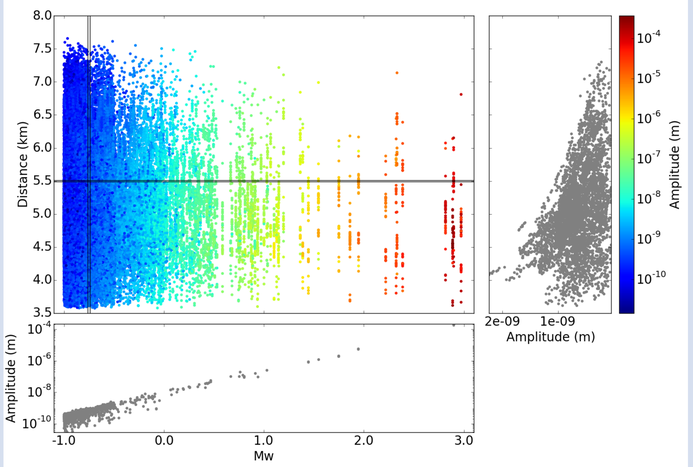

Figure 4. *Maximum amplitudes according to the hypocentral distance for each station and the moment magnitude are plotted for the complete synthetic microseismic catalogue. Amplitude profiles are plotted for hypocentral distance 5.5 km and moment magnitude Mw -0.75.*

4. DETECTION PERFORMANCE AND MAGNITUDE OF COMPLETENESS

To reproduce true monitoring conditions at the different station locations, we add real noise to synthetic traces. The detection probability for different magnitudes and source-receiver distances is estimated based on average noise amplitude for each station (figure 5). This information is used to estimate the detection performance of the network (requiring simultaneous detection by 5 sensors) and the magnitude of completeness at the depth of the hydraulic fracturing horizontal wells (figure 6).

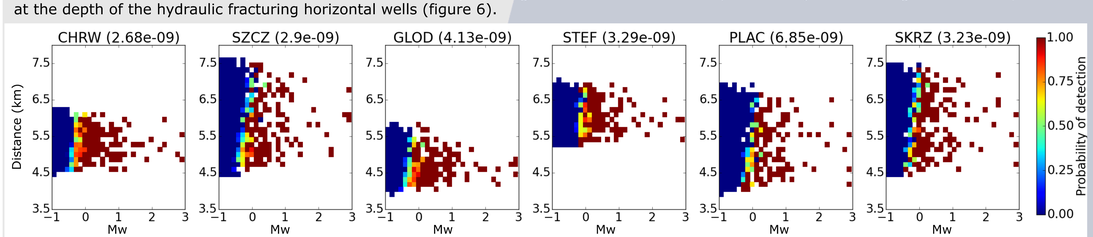

Figure 5. *Probability of detection for each broadband station. We estimated an average value for the real noise amplitude (see plot title for each station). Events are assumed to be detected if the maximum amplitude is greater than the average noise value.*

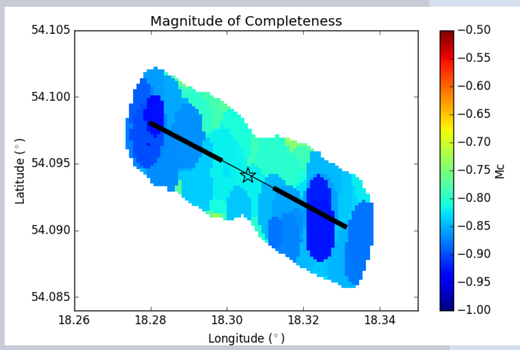

Figure 6. *Estimated magnitude of completeness in the fracking area. Black lines show the fracking drillings.*

5. DISCUSSION & CONCLUSIONS

Our technique is useful to evaluate the efficiency of the seismic network and validate detection and location algorithms, taking into account the signal to noise ratio. The same dataset may be used at a later time, to assess the performance of other seismological analysis, such as hypocentral location, magnitude estimation and source parameters inversion.

REFERENCES & ACKNOWLEDGEMENTS

Baig, A., and T. Urbancic (2010). Microseismic moment tensors: A path to understanding frac growth: The Leading Edge, 29, 320–324.

Grad, M., M. Polkowski, and S. R. Ostaficzuk (2015). High-resolution 3D seismic model of the crustal and uppermost mantle structure in Poland. Tectonophysics, 666, 188-210.

Kwiatek, G., K. Plenkers, and G. Dresen (2011). Source parameters of picoseismicity recorded at Mponeng deep gold mine, South Africa: Implications for scaling relations, Bull. Seismol. Soc. Am., 101, 2592–2608.

Madariaga, R. (1976). Dynamics of an expanding circular fault, Bull. Seismol. Soc. Am. 66, 639–666.

This work is funded by the **EU H2020 SHEER project**.

www.gfz-potsdam.de